Uplink Performance Enhancement Through Adaptive Multi Association and Decoupling in UHF mmWave Hybrid_Networks

DOI:
10.1109/TVT.2019.2932691

Document Version
Accepted author manuscript

Uplink Performance Enhancement Through Adaptive Multi-Association and Decoupling in UHF-mmWave Hybrid Networks

Yao Shi, *Student Member, IEEE*, Emad Alsusa, *Senior Member, IEEE*, Aysha Ebrahim, *Member, IEEE* and Mohammed W. Baidas, *Senior Member, IEEE*

***Abstract*—The rapid increase of wireless applications and services coupled with the arrival of 5G and Internet of Things will not only exacerbate demand for further capacity at the downlink (DL) but also crucially at the uplink (UL). One of the most potential enablers to simultaneously optimize both links is the DL/UL decoupling (DUDe) technique which does so by exploiting the possibility of associating each user to a different base station (BS) in each link direction. Moreover, the increasing desire to incorporate millimeter-wave (mmWave) communications in future networks further enriches the possibilities to achieve higher capacities. To this end and in contrast to existing works which use dual association based on minimum path-loss (Min-PL), this paper investigates the merits of adopting capacity-based multi-association in ultra-high frequency (UHF) and mmWave hybrid networks, where mobile users may simultaneously connect to multiple UHF small cells (SCells), millimeter-wave SCells and/or UHF macro cells (MCells). It will be shown that, our joint association and resource management approach can provide higher data rates and energy efficiency than many benchmark techniques. To achieve an insight into the performance of the proposed design, the results present a comprehensive comparison based on single and multi-connectivity as well as coupled and decoupled association for a variety of important metrics.**

***Index Terms*—Heterogeneous networks, cell association, downlink/uplink decoupling, millimeter-wave, dual connectivity**

I. Introduction

MANY 3G and 4G mobile communication services were created for users to consume content rather than generate it. Thus, the network traffic in the downlink (DL) tended to be much larger than that in the uplink (UL). As such, traditional networks were designed to mainly maximize the DL capacity. However, with the rise of a new trend of user-centric wireless services and applications, the demand on the UL capacity is expected to intensify [1].

In traditional homogeneous networks, only macro-cells (MCells) with similar wireless transmission characteristics (e.g. base-station (BS) type, coverage, topology, frequency band, etc.) are deployed. The main strategies to increase network capacity in such networks are to increase the number of macro BSs and expand transmission bandwidth. However, it is not always possible to add more MCells to existing cellular networks due to the excessive operational and capital expenditures or/and lack of suitable sites (e.g. in crowded public places and harsh terrain). Thus, the more flexible, low-cost, low-complexity, and short-range small cells (SCells), such as picocells and femtocells, are introduced into the network. Particularly, SCells are added to improve network capacity in areas not covered by the MCells (i.e. cellular coverage range extension), and also to meet the high data rate user demands and service quality by offloading from the large macro network. Furthermore, the coexistence of MCells and SCells can significantly reduce energy consumption by shortening the distance between the UEs and their serving base-stations. Multi-tiered networks that overlay MCells and SCells (i.e. BSs with varying types, sizes and transmission characteristics) are called heterogeneous networks (HetNets). HetNets can bring advantages over conventional homogenous networks in meeting the demand for mobile network capacity, coverage and energy-efficiency. The specifications of the different elements in HetNets are shown in Table I [2]. As there is a clear disparity between the transmit powers of the MCells and SCells, the best serving cell per user may only be so in one link direction; hence, if the UL and DL associations are coupled, the UL capacity may be severely penalized. A potential solution to alleviate such a predicament is the DL/UL decoupling (DUDe) technique [3], which allows users to connect to different BSs in the UL and DL to maximize the link capacity in each direction. DUDe not only shortens the distance between the user equipments (UEs) and serving BSs, but also makes better use of the spectral resources of small BSs. To do so, the authors in [3] have proposed a minimum path-loss (Min-PL) scheme and quantified the potential throughput gain using real data from Vodafone's LTE network. The analytical joint rate and signal-to-interference-plus-noise ratio (SINR) coverage for decoupled uplink-downlink biased

TABLE I: Specifications of Different Elements in HetNets

Types of nodes	Transmit power	Coverage	Backhaul
Macrocell	46dBm	Few km	S1 interface
Picocell	23-30dBm	<300m	X2 interface
Femtocell	<23dBm	<50m	Internet IP
Relay	30dBm	300m	Wireless

Yao Shi and Emad Alsusa are with the School of Electrical and Electronic Engineering, University of Manchester, Manchester M1 3WE, UK (e-mail: yao.shi@manchester.ac.uk, e.alsusa@manchester.ac.uk).

Aysha Ebrahim is with the Information Technology Department, University of Bahrain Sakhir Campus, Sakhir 32038, Bahrain (e-mail: amebrahim@uob.edu.bh).

Mohammed W. Baidas is with the Electrical Engineering Department, College of Engineering and Petroleum, Kuwait University, Kuwait (e-mail: Baidas@ieee.org).

cell associations in HetNets were presented in [4], while the association probability based on stochastic geometry were derived in [5]. The UL performance improvement brought by DUDe was theoretically investigated in [6].

On the other hand, as wireless communications are reaching the bottleneck of insufficient traditional spectrum resources, millimeter-wave (mmWave) frequency spectrum is envisaged to offer an essential lifeline for future broadband cellular systems in the quest to satisfy the anticipated explosive resources demands. However, due to the directional transmission of mmWave, where the multi-user interference may fall precipitously, mmWave systems are noise-limited [7,8]. Nonetheless, the smaller wavelength of mmWave signals enables proportionally greater antenna gain for the same physical antenna array [7]. That said, the propagation characteristics, such as high near-field path-loss, severe oxygen and water molecules absorption, pose great challenges. Fortunately, recent research shows that these problems can be overcome using highly directional antennas and beamforming techniques [9,10], but this does not mean that mmWaves alone can help achieve universal coverage, especially in high blockage areas. Thus, using mmWave BSs with ultra-high frequency (UHF)[1] BSs is an appealing approach, particularly when combined with DUDe. A recent study in [12] showed that to satisfy acceptable exposure limits at frequencies above 6 GHz, the maximum transmit power in the UL should be several dBs below the power levels used in current cellular technologies. Although the SNR can be maintained by mounting antenna arrays on the BS, it is also possible to achieve this by shortening the distance between BSs and UEs to reduce the path-loss. Nonetheless, mmWave signals tend to experience lower SNRs, as the mmWave bandwidth is much wider than UHF bandwidth and the transmit power per Hertz for mmWave is much lower than UHF. A number of studies have examined the application of DUDe in mmWave-UHF hybrid networks including, e.g. [13], in which the authors have derived the SINR and rate distributions from path-loss based and capacity-based cell association perspectives. Also, in [14], O. W. Bhatti et al. analyzed the performance of DUDe in such networks using real blockage data. Moreover, allowing a user to be simultaneously served by multiple BSs is another viable approach to satisfy the user's data requirements [15,16]. In the case of dual connectivity (DC) for instance, each UE is allowed to simultaneously utilize the spectrum from two BSs connected together via non-ideal backhaul links. In such scenarios, the information can be either split or transmitted twice. This network architecture with functionality separation is estimated to save more than one-third of the current overall network power consumption [17]. However, as the transmit power of UEs is limited, adopting this in the UL could be counterproductive unless combined with DUDe to make it more power efficient. The technical challenges imposed by this approach and the potential solutions are discussed in [18,19].

[1]UHF refers to the radio frequencies in the range between 300 MHz and 3GHz. Most frequencies used in mobile 4G network are classified in the UHF band [11].

A. Main Contributions

There have been many studies on decoupling, but most of which are based on Min-PL cell association schemes. Additionally, although there is a strong upward trend focusing on mmWave communication and dual connectivity, to the best of our knowledge, networks with dual connectivity where BSs transmit over both mmWave and UHF bands have not been considered before. In turn, this paper investigates the feasibility of mmWave with DUDe in HetNets. In particular, we focus on decoupling the UL and DL serving BSs from the perspective of maximizing the total network capacity. To this end, we propose an efficient joint resource-management and cell-association technique for hybrid HetNets, and compare its performance for a wide range of metrics with benchmark single and dual connectivity alternatives. Specifically, we investigate the performance of single and dual connectivity techniques in both path-loss based and capacity-based approaches in three-tier UHF-mmWave hybrid network, where mmWave SCells, UHF SCells and MCells coexist. For comparison, the special case where all SBSs are of the same type is also considered. To evaluate the potentials of capacity-based cell association scheme, we formulate the problem of joint cell association and network capacity maximization as a mixed-integer nonlinear programming problem, which serves as an upper-bound benchmark of the network capacity. Besides, the complexity and energy efficiency analyses of the proposed technique are also provided.

B. Organization

The rest of this paper is organized as follows. In Section II, the assumptions considered in the system model are explained. In Section III, the proposed joint resource-management and cell-association technique with decoupling capability is presented. In Section IV, the performance of path-loss based and capacity-based cell association schemes are evaluated in the single and dual connectivity scenarios. Finally, Section V concludes the paper.

II. System Model

We consider an orthogonal frequency-division multiple access (OFDMA) HetNet with UHF MCells, UHF SCells, mmWave SCells and UEs following independent homogeneous Poisson Point Processes (HPPP) Φ_m, Φ_{s_1}, Φ_{s_2} and Φ_u with intensities λ_m, λ_{s_1}, λ_{s_2} and λ_u, respectively. The ratio of the SCell density to the MCell density is denoted by β, while the ratio of UHF SCells to all SCells is denoted by γ. The user traffic is based on the full-buffer model.

A. Cell Association Model

We consider macro base stations (MBSs) transmitting over UHF bands, and small base stations (SBSs) transmitting over UHF or mmWave bands. It is also assumed that the UEs can connect to any type of BSs and are capable of operating at UHF and mmWave bands. Also, each UE can connect to one BS or two BSs over different sub-carriers. In the DL, the UEs connect to the best one or two BSs according to the biased

reference signal received power (RSRP) criterion [20,21]. If the UL and DL are coupled, the UEs connect to the same BSs in both link directions; otherwise, the UL BSs will be separately selected using the path-loss based association in [3], or the capacity-based association proposed in this paper. It is worth emphasizing that the UE can connect up to 2 BSs on each link direction simultaneously (i.e. 4 BSs in total). While it is possible to allow each UE to be associated with more than two BSs for each link direction, it was found that the resulting improvement in sum-rate is negligible. This is because the potential capacity gain for the UEs connecting to more than two BSs is more often outweighed by the amount of interference caused to adjacent BSs; ultimately leading to an overall capacity reduction. Furthermore, complexity significantly increases, as the more BSs a UE is connected to, the more overhead is generated, adding to the side-information to be processed.

The core idea of capacity-based association is to adaptively switch between coupling and decoupling the UL and DL on the basis of maximizing capacity at each link; similarly for when adapting between single and dual connectivity. This association scheme will be further explained in Section III, while in this section, we will briefly describe the Min-PL based association scheme.

In the Min-PL criterion, the UEs are connected to the BS with the lowest path-loss [3,19]. A typical UE is associated with BS l in the UL if and only if

$$P_u W_l {L_l}^{-1} \geq P_u W_k L_{min,k}^{-1}, \quad \forall k, l \in \{s_1, s_2, m\}, \tag{1}$$

where P_u is UE's transmit power, W is the UL cell bias value which is positive referring to expanding the coverage of the cells, L_l is the UL path-loss of the typical UE to the BS l, and $L_{min,k} = \min_{x \in \Phi_k} L_k(x)$ is the minimum UL path-loss of the typical UE to the k^{th} tier BS.

B. Uplink and Downlink Interference Model

The system bandwidth is equally divided into N orthogonal resource blocks (RBs), where each RB is divided into 12 resource elements (REs). Each RE refers to a subcarrier. The subcarrier spacing is 15 kHz for UHF and 60 kHz for mmWave. UEs in the same cell occupy orthogonal RBs, so there is no intra-cell interference, but UEs in different cells interfere with each other. Moreover, there is no interference between UHF and mmWave cells as their frequency bands are orthogonal. The DL SINR between UE k and its serving BS i at RB n is given by

$$\eta_{i,k,n} = \frac{\Gamma_{i,n} \hbar_{i,k,n} L_{i,k,n}^{-1}}{\eta_0 + \sum_{j=1}^{B} \Gamma_{j,n} \hbar_{j,k,n} L_{j,k,n}^{-1}}, \quad j \neq i, \tag{2}$$

where $\Gamma_{i,n}$ is the transmit signal power of the BS i at the RB n, $\hbar_{i,k,n}$ is Rayleigh fading channel for UHF signals and Rician fading channel for mmWave signals. The K-factor is set to be 7dB for LOS and 6dB for NLOS [22]. The number of paths is 10. The adopted multipath channel model is the same as [23]. $L_{i,k,n}$ is the path-loss, $\sum_{j=1}^{B} \Gamma_{j,n} \hbar_{j,k,n} L_{j,k,n}^{-1}$ is the interference power (for $j \neq i$), B is the number of BSs and η_0 is the power of additive white Gaussian noise (AWGN). On the other hand, the UL SINR is given by

$$\eta_{k,i,n} = \frac{\Gamma_{k,n} \hbar_{k,i,n} L_{k,i,n}^{-1}}{\eta_0 + \sum_{l=1}^{K} \Gamma_{l,n} \hbar_{l,i,n} L_{l,i,n}^{-1}}, \quad l \neq k, \tag{3}$$

where $\Gamma_{k,n}$ is the transmit signal power of UE k at RB n , K is the number of UEs and $\Gamma_{l,n}$ is the transmit power of other UEs.

C. Resource Allocation

Resource allocation is performed using the aperiodic channel quality indicator (CQI) [24] reported from the UEs. In LTE and LTE-A systems, the CQI is often used for packet scheduling (PS). Specifically, PS refers to selecting the scheduling time and frequency for each UE. UEs report the CQI value for each RB to their serving BS. The BSs utilize these CQI reports to select the preferred RBs for each UE. The CQI report from a given UE includes information regarding the SINR for each physical RB from the received pilot power and total interference every measurement period.

D. Propagation Model

The path-loss $L(d)$ is modeled as

$$L(d) = 20 \log \left(\frac{4\pi f}{c} \right) + 10\theta \log(d) + \chi, \tag{4}$$

where d is the distance between the UEs and BSs, f is the operating frequency, c is the light speed, θ is the path-loss exponent, and χ is the zero-mean log normal shadowing. Line-of-sight (LOS) mmWave, none-line-of-sight (NLOS) mmWave and UHF links have different values of θ and χ. We adopt the same blockage model as in [25]. If the distances between the users and mmWave SCells are less than the threshold μ = 200 m, then these links are assumed LOS with probability ω = 0.2, otherwise, these links are assumed NLOS. The parameters μ and ω are environment-dependent.

It is assumed that the UHF BSs are equipped with omni-directional antennas, the mmWave BSs are equipped with directional antenna arrays to compensate for the high path-loss, and the UEs are equipped with omni-directional antennas [13,25]. The antenna gain at a mmWave BS is formulated by

$$G_b(\theta) = \begin{cases} G_M, & |\theta| \leq \theta_b/2, \\ G_m, & \text{otherwise}, \end{cases} \tag{5}$$

where $\theta_b = 10^\circ$ is the beamwidth of the main lobe, G_M = 18dBi and $G_m = -2$dBi denote the gains of main lobe and side lobe, respectively. The mmWave UEs are assumed to be in perfect alignment with their serving cells, while the beam directions of interfering mmWave links are independently and uniformly distributed in $[-\pi, \pi]$. Moreover, the antenna gain of an interfering mmWave link is G_M with a probability of $p_M = \theta_b/2\pi$, and is G_M with a probability of $p_m = 1 - p_M$.

E. Energy Efficiency Model

As DUDe will not affect DL cell association, and the BSs are generally assumed to have an abundance of power supply, we only consider the energy efficiency (EE) in the UL [26], which is defined as

$$EE = \frac{\sum_{u\in\Phi_u}\tau_u}{\sum_{u\in\Phi_u}P_u}, \tag{6}$$

where τ_u is the data rate of UE u, P_u is the UL transmit power of UE u. P_u (expressed in dBm) can be written as [27,28]

$$P_u = \min\{P_{\max}, 10\log_{10}M + \alpha\tilde{L} + P_0 + \Delta_{mcs}\}, \tag{7}$$

where $P_{\max}$ is the maximum transmit power of UEs, P_0 is the power baseline value reflecting the noise level in the UL, Δ_{mcs} is a parameter which depends on the modulation and coding scheme chosen, M is the number of RBs assigned to the UE, $\alpha \in \{0, 0.4, 0.5, 0.6, 0.7, 0.8, 0.9, 1\}$ is a compensation factor for $\tilde{L}$, which is the total UL signal loss, including path-loss, shadowing, fast fading, etc.

III. Capacity-Based Cell Association

In this section we describe the proposed capacity maximization approach. Due to the random nature of the user positions, some BSs may occasionally be highly loaded while others are underutilized. Moreover, the high path-loss of mmWaves makes them often less favorable to UEs than UHF BSs even though they offer much more bandwidth. To increase the participation of mmWave SBSs, association schemes that maximize frequency reuse and capacity should be sought. To this end, we extend the joint network capacity and QoS Maximization (NCQM) method presented in our previous work for conventional HetNets [29] to the case of hybrid-networks with DUDe. Specifically, we refine the criteria and adapt it to encompass the new dimensions of the considered network including dual connectivity and mmWave-BSs. The presented scheme can be divided into two parts. The coupling/decoupling association (CDA) part determines when to decouple the UL and DL, while the single/multi-BS association (SMBA) part determines when to select dual connectivity over single connectivity per user per link. Using this scheme, some UEs are offloaded to the BSs which can provide more RBs rather than those with lower path-loss.

A. Coupling/Decoupling Association

In the UL, UEs are initially connected to the same BSs as those in the DL. It is worth noting that one UE can connect to one or two BSs. Thus a association and interference matrix $\Theta \in \mathbb{R}^{B\times K}$ can be constructed as

$$\Theta_{i,k} = \begin{cases} 2, & \text{UE } k \text{ is connected to BS } i, \\ 1, & \text{if } P_{i,k} > \eta_0 + \sigma, \\ 0, & \text{otherwise,} \end{cases} \tag{8}$$

where $P_{i,k}$ is the UL interference power, σ is the interference threshold and η_0 is the noise power, $\Theta(i,k)$ represents the relation between UE k and BS i, as follows: a) UE k is served by BS i ($\Theta(i,k) = 2$); b)UE k interferes with BS i ($\Theta(i,k) = 1$); and c) UE k do not interfere with BS i ($\Theta(i,k) = 0$). Since there are N RBs overall, the average number of RBs that BS i can provide to each UE is given by

$$\Omega_i = \left\lfloor \sum_{k=1}^{K}\{\Theta_{i,k} = 1\} + \sum_{k=1}^{K}\{\Theta_{i,k} = 2\} \right\rfloor, \tag{9}$$

If UE k can get Ω_i and Ω_j RBs from its serving BS i and a neighboring BS j separately, then a candidate pair matrix $\Lambda \in \mathbb{R}^{B\times K}$ can be constructed as

$$\Lambda_{j,k} = \begin{cases} 1, & \Omega_j > \Omega_i,\ i \neq j \\ 0, & \text{otherwise.} \end{cases} \tag{10}$$

If $\Lambda(j,k) = 1$, then UE k and BS j is a candidate link. With this in mind, the achievable capacity for each $\Lambda_{j,k}$ is obtained as

$$C_{j,k} = \sum_{n\in\beta_{j,k}} W\log_2(1+\gamma_{k,j,n}), \tag{11}$$

where W is the bandwidth of each RB, $\beta_{j,k}$ is the index of RBs occupied by the association pair (j,k), and its length is Ω_j. If $C_{j,k} > C_{i,k}$, then the overall network capacity can be determined as

$$C_{tot} = \sum_{j=1}^{B}\sum_{k=1}^{K}\sum_{n\in\beta_{j,k}} W\log_2(1+\gamma_{k,j,n})\}. \tag{12}$$

The candidate pair with the highest overall network capacity will replace the original association pair (i,k). This algorithm is guaranteed to converge when it cannot find any more pairings that would improve the overall capacity. The steps above are formulated in a pseudo-code structure in Algorithm 1.

As the capacity for each candidate pair and the overall network capacity need to be calculated many times, the time complexity of this association scheme can be higher than that of Min-PL. According to [30], the time-complexity of the Shannon capacity formula is unknown, therefore we assume it to be $O(1)$. Assuming the number of candidate pairs and deployed UEs are given by K_a and K_b respectively, and the number of candidate pairs satisfying $C_{j,k} > C_{i,k}$ is K_c, then the computational complexity of this scheme is expressed as $(K_c+1)K_bO(1) + K_aO(1) = (K_cK_b + K_b + K_a)O(1)$. Parameters K_a and K_c increase with the number of BSs and UEs.

B. Single/Multi-BS Association

The association scheme in this part is different from the dual connectivity association scheme in [19] in the sense that UEs can connect to one more BS if higher capacity can be achieved. Only a small portion of the UEs may be connected to two BSs, and thus UEs can connect in a single or dual hybrid connectivity. Assuming UE u is connected to BS j, and BS f is its neighbouring BS, then UE u may also connect to BS f if conditions C1, C2 and C3 are all satisfied, which are stated as follows.

C1: The additional RBs from BS f do not overlap with the existing RBs provided by BS j as follows

$$\delta_{f,u} + \delta_{j,u} < N, \tag{13}$$

Algorithm 1 Coupling/Decoupling Association (CDA)

Initialization: calculate Θ, Ω_i, Ω_j and current network data rate $C_{tot}^{'}$;
Set $C_{tot} = C_{tot}^{'}$;
for $k = 1$ until K **do**
  $\omega = (0, 0)$;
  for $i = 1$ until B **do**
    if $\Theta_{i,k} = 2$ **then**
      Calculate $C_{i,k}$;
    end if
    for $j = 1$ until B **do**
      if $\Theta_{j,k} = 1$ & $\Omega_j > \Omega_i$ **then**
        $\Lambda_{j,k} = 1$ and calculate $C_{j,k}$;
        if $C_{j,k} > C_{i,k}$ **then**
          Calculate the updated network data rate $C_{tot}(j,k)$ with the candidate association pair (j,k);
          if $C_{tot}(j,k) > C_{tot}$ **then**
            $C_{tot} = C_{tot}(j,k)$;
            $\omega = (j,k)$;
          else
            Reject the candidate association pair (j,k);
          end if
        end if
      end if
    end for
  end for
  if $\omega \neq (0,0)$ **then**
    Replace the original association pair (i,k) with ω;
    Recalculate Θ, Ω_i, Ω_j;
    Set $C_{tot}^{'} = C_{tot}$;
  end if
end for

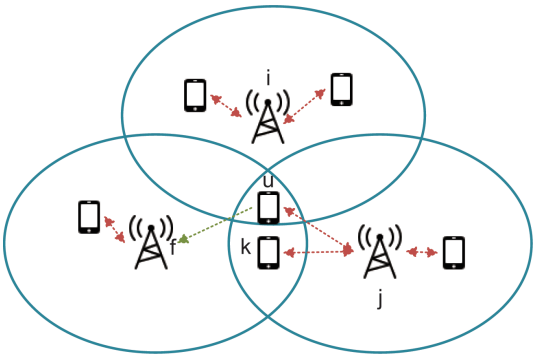

Fig. 1: Illustration of SMBA association scheme.

where $\delta_{f,u}$ and $\delta_{f,u}$ are the numbers of RBs from BSs f and j separately. If BSs j and f are in different frequency bands, i.e., UHF and mmWave, there is no need to check this condition.

C2: The second connection does not interfere with any other BS (BS i, j and f in Fig. 1) that covers UE u within its area, as follows

$$\phi + \delta_{f,u} + \delta_{j,u} < N, \tag{14}$$

where ϕ is the number of RBs occupied by BS i or j. Similar

Algorithm 2 Single/Multi-BS Association (SMBA)

Initialization: calculate Θ, Ω_i, Ω_j and current network data rate $C_{tot}^{'}$;
Set $C_{tot} = C_{tot}^{'}$;
for $k = 1$ until K **do**
  $\omega = (0, 0)$;
  for $i = 1$ until B **do**
    for $j = 1$ until B **do**
      if $\Theta_{j,k} = 1$ & C1 & C2 & C3 **then**
        Calculate the updated network data rate $C_{tot}(j,k)$ with the candidate association pair (j,k) added;
        if $C_{tot}(j,k) > C_{tot}$ **then**
          $C_{tot} = C_{tot}(j,k)$;
          $\omega = (j,k)$;
        else
          Reject the candidate association pair (j,k);
        end if
      end if
    end for
  end for
  if $\omega \neq (0,0)$ **then**
    Add the original association pair ω;
    Recalculate Θ, Ω_i, Ω_j;
    Set $C_{tot}^{'} = C_{tot}$;
  end if
end for

to C1, BSs i, f, and j may be in different frequency bands, and UEs transmit over different bands will not interfere with each other.

C3: The second connection does not interfere with any UE (UE k in Fig. 1) interfered by BS f, as follows

$$\phi_f + \delta_{f,u} + \lambda_k < N, \tag{15}$$

where ϕ_f and λ_k are the numbers of RBs already occupied by BS f and UE k, separately. The achieved capacity for each candidate pair satisfying all the conditions is calculated according to (13) and the priority of selection is given to the candidate pair with the highest capacity. This process repeats until the overall capacity in (14) cannot be increased any more, so this algorithm is also convergent. These steps are formulated in a pseudo code structure in Algorithm 2. Assuming the number of candidate pairs that satisfy all the conditions is K_s, then the computational complexity can be expressed as $(K_s + 1)K_b O(1)$, where the parameter K_s increases with the number of BSs and UEs.

The DUDe technique and our proposed schemes have some impact on the network architecture and signaling overhead. For instance, a central unit is necessary to collect the information from all BSs in the group[2] and calculate the parameters needed in our algorithm, such as how many UEs are within the coverage area of each BS in the UL, the number of allocated resources per UE, and the path-loss of each link, so that the

[2]A group consists of one, or several, MBSs and some SBSs.

central unit can control the BS handover. Besides, the UL-related control signaling needs to be transmitted from the DL node, while the DL-related control signaling from the UE needs to be received by the UL node, and forwarded to the DL node over the network infrastructure [1].

To construct the association and interference matrix Θ, each BS needs to send its local association and interference map Θ_i to the central unit. If we assume there are B BSs in the coverage of the central unit, BS i has K_i users, and the number of bits needed to encode $\Theta_{i,k}$ is D, then the total number of bits required for all the BSs to forward Θ_i to the central unit is $\sum_{i=1}^{B} K_i D$.

C. Joint Cell Association and Network Capacity Maximization

The capacity-based association schemes (CDA&SMBA) do not necessarily guarantee global optimal network capacity. In order to quantify the upper-bound of the UL network sum-rate, the problem of joint cell association and network capacity maximization (J-CA-NC-MAX) is formulated as a mixed integer nonlinear programming problem. Particularly, the aim is to associate the K UEs with the B BSs, such that each UE is associated with at least (most) ρ (ψ) BSs in the UL. Also, the sum of transmit powers of the UEs associated with each BS must satisfy $P_{\max}$. The J-CA-NC-MAX problem is formulated as

J-CA-NC-MAX

$$\max \quad C_{tot} = \sum_{j=1}^{B}\sum_{k=1}^{K}\sum_{n\in\beta_{j,k}} W\log_2(1+\gamma_{k,j,n})\}, \tag{16a}$$

$$\text{s.t.} \quad \sum_{k=1}^{K} I_{j,k}P_{j,k} \le P, \quad \forall j \in \{1,2,\ldots,B\}, \tag{16b}$$

$$\sum_{j=1}^{B} \mathcal{I}_{j,k} \le \psi, \quad \forall k \in \{1,2,\ldots,K\}, \tag{16c}$$

$$\sum_{j=1}^{B} \mathcal{I}_{j,k} \ge \rho, \quad \forall k \in \{1,2,\ldots,K\}, \tag{16d}$$

$$0 \le P_{j,k} \le P, \quad \forall k \in \{1,2,\ldots,K\}, \forall j \in \{1,2,\ldots,B\}, \tag{16e}$$

$$\mathcal{I}_{j,k} \in \{0,1\}, \quad \forall k \in \{1,2,\ldots,K\}, \forall j \in \{1,2,\ldots,B\}, \tag{16f}$$

where $\beta_{j,k}$ is the index of RBs occupied by the association pair (j, k), while $I_{j,k}$ is a binary decision variable, defined as

$$\mathcal{I}_{j,k} = \begin{cases} 1, & \text{if UE } k \text{ is associated with BS } j, \\ 0, & \text{otherwise.} \end{cases} \tag{17}$$

In this work, it is assumed that each UE is associated with at least one BS and at most two BSs (i.e. $\rho = 1$ and $\psi = 2$). Lastly, it should be noted that the J-CA-NC-MAX problem is non-convex, and thus is computationally-intensive and time-consuming even for moderate size of networks (i.e. not practical). However, it is considered in this work as an upper-bound benchmark for the network capacity. The J-CA-NC-MAX is solved via MIDACO, with tolerance set to 0.001 [31].

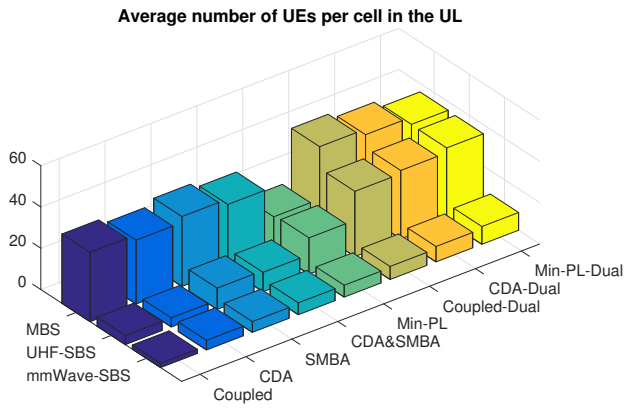

Fig. 2: Average number of UEs per cell in the UL for different association schemes in single and dual connectivity scenarios ($\beta = 2$, $\gamma = 0.5$).

IV. Performance Analysis

In this section, the performance of the proposed schemes in both single and dual connectivity scenarios are evaluated and compared with the state-of-the-art alternatives. The 5G NR frame structure supports both TDD and FDD transmissions, but for the mmWave band, it only supports TDD at present [34]. Thus, TDD is applied in this paper. We assume half of the time is used for the UL and we do not consider the overhead due to switching between transmission directions. We know that the network traffic in the DL tends to be much larger than that in the UL, but we believe that with the rise of new services and applications of 5G and IoT, the UL transmission is expected to increase [1]. Besides, DUDe increases the UL data rate without impacting the DL data rate; thus, only the UL data rate is considered in this paper. In the dual connectivity scenario, we consider at most two uplink associations. For the Min-PL scheme, UEs can connect to the first and second best serving BSs with the lowest path-loss. In the case of the SMBA scheme, UEs can connect to one more BS if higher capacity can be achieved from the decoupling. The list of all the association schemes are shown in Table II, while the simulation parameters are listed in Table III. To analyze the improvements, data rate and load situations in the MCells and SCells have been selected as metrics. Monte Carlo simulation is utilized to evaluate the different association and connectivity schemes.

A. Three-Tier HetNet

We consider three-tier UHF-mmWave hybrid networks first, where mmWave SCells, UHF SCells and MCells coexist.

TABLE II: Cell Association Schemes

Conectivity	Coupled association	Decoupled association
Single	Coupled (biased RSRP)	Min-PL, CDA, SMBA, CDA&SMBA
Dual	Coupled-Dual (biased RSRP)	Min-PL-Dual, CDA-Dual

TABLE III: Simulation Parameters

Parameters	UE	MCell	UHF SCell	MmWave SCell
Maximum transmit power	23 dBm	46 dBm	30 dBm	30 dBm
Downlink/Uplink bias	N/A	0/0 dB	3/0 dB	5/0 dB
Spatial distribution	Poisson point process			
Spatial density	250 per km^2	5 per km^2	$\gamma\beta\lambda_m$	$(1-\gamma)\beta\lambda_m$
Lognormal shadowing	N/A	$\mu = 0$, $\sigma = 4$ dB	$\mu = 0$, $\sigma = 4$ dB	LOS $\mu = 0$, $\sigma = 8.66$ dB, NLOS $\mu = 0$, $\sigma = 9.02$ dB [7]
Path-loss exponent	N/A	3	3	LOS 2.55, NLOS 5.76 [7]
Operating frequency	N/A	2 GHz	2 GHz	28 GHz
Bandwidth	N/A	20 MHz	20 MHz	200 MHz [32]
Subcarrier spacing	N/A	15 kHz	15 kHz	60 kHz [32]
OFDM symbol period	N/A	66.67 us	66.67 us	16.67 us [33]
Power control	Transmit at the maximum power level			
Noise density	-174 dbm/Hz			

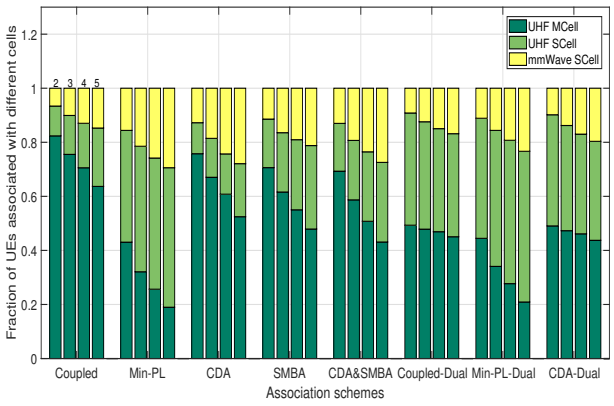

Fig. 3: Ratio of UEs associated with different BSs at different ratios of SCell density to MCell density and association schemes ($\gamma = 0.5$).

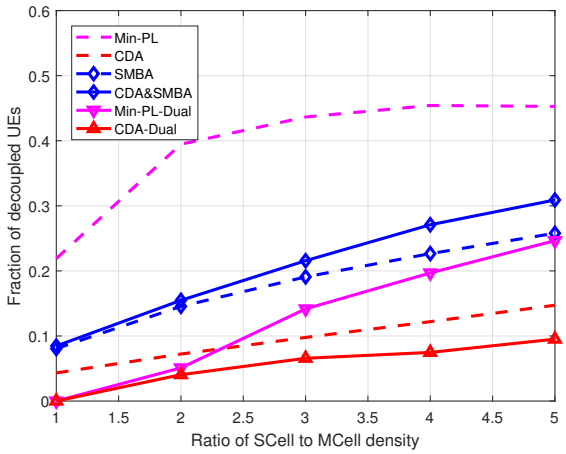

Fig. 4: Ratio of UEs decoupled in the UL and DL vs. ratio of SCell density to MCell density ($\gamma = 0.5$).

Fig. 2 illustrates the average number of UEs per cell in the UL for the different association schemes. The figure reveals that the decoupled association schemes offload more UEs to underutilized SCells in the UL direction, and thus potentially freeing more MCell resources for users out of SCell coverage. Additionally, although the numbers of mmWave and UHF SCells are equal, it is obvious that more UEs connect to UHF SCells. This is because the path-loss of mmWave signals is higher, and there may be no LOS link between the BSs and UEs. Even if the directional antenna array is applied, as the mmWave bandwidth is much wider than UHF bandwidth, the transmit power per Hertz for mmWave is much lower than UHF, and thus it will also decrease the SNR. Besides, compared with the capacity-based (CDA, SMBA) association schemes, the receive signal power based (Min-PL) association scheme provides higher probability for the UEs to connect to the small BSs (SBSs) in both single and dual connectivity scenarios. The reason is that in the CDA and SMBA schemes, UEs initially connect to the same BSs as those in the DL.

Fig. 3 shows the fraction of UEs associated with MCells, UHF SCells and mmWave SCells in the UL direction at various SCell to MCell densities. The numbers 2, 3, 4, 5 on the top of bars refer to the different ratios of SCells to MCells density. In general, decoupling schemes make use of a bigger proportion of SCells, which in turn results in an increase of SCell UEs. For the coupled association scheme and CDA scheme, the ratio of association pairs with MBSs in dual connectivity is lower than that in single connectivity. This is because the number of MBSs is much lower than that of SBSs and most UEs are associated with MCells in the DL, in the case when there is only one MBS nearby, then the second association pair must be with an SBS. Accordingly, the ratio of association pairs with UHF SBSs in dual connectivity is higher than that in single connectivity, but the ratio of association pairs with the mmWave SBSs in the dual connectivity scenario is almost the same as that in the single connectivity scenario, which is because of the severity of the near-field path-loss of mmWaves. In other words, the UEs prefer UHF SBSs to mmWave SBSs when both are available.

Fig. 4 shows the DUDe ratio at various SCell to MCell density ratios. When the SCell density increases, there will be more overlapped regions, which provides more flexibility for users to be handed-off to less loaded cells, and hence the number of DUDe UEs increases. Moreover, the DUDe ratio becomes lower when each UE connects to two BSs. For CDA and SMBA, as their initial association pairs are the same as those in the UL, their DUDe ratios tend to be lower. In contrast, the UL association pairs based on Min-PL are independent and experience a higher DUDe rate in single and dual connectivity scenarios. It also explains why based on

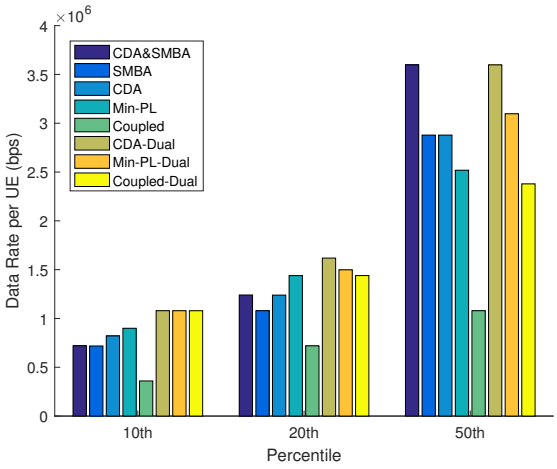

(a) 10th, 20th, 50th percentile data rates

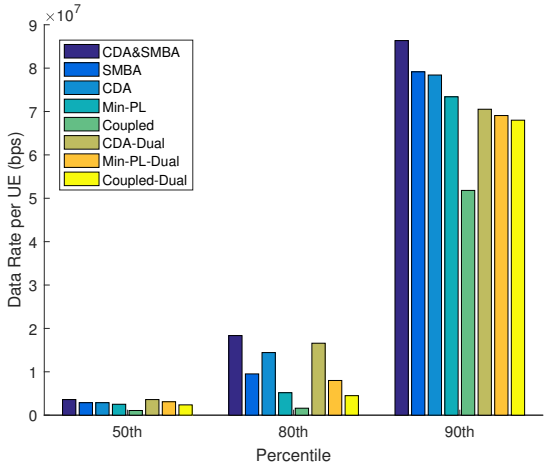

(b) 50th, 80th, 90th percentile data rates

Fig. 5: 10th, 20th, 50th, 80th, 90th percentile UE UL data rates based on different cell association schemes in single and dual connectivity scenarios ($\beta = 5, \gamma = 0.5$).

Min-PL more UEs connect to SBSs in Fig. 3.

Figs. 5a and 5b show the 10th, 20th, 50th, 80th, 90th percentile UE UL data rates based on eight cell association schemes. A percentile is a measure used in statistics indicating the value below which a given percentage of observations in a group of observations fall [35]. For example, the 20th percentile is the value (or score) below which 20% of the observations may be found. Because of the wide bandwidth of mmWave, a few UEs associated with mmWave SBSs have extremely high data rates, and so the 80th and 90th percentile data rates are extremely high. The data rate based on the coupled scheme is the lowest in both single and dual connectivity scenarios. This can be explained by the fact that higher coverage of SCells in the DUDe cases results in a better distribution of UEs among the nodes, which provides better utilization of the resources. Additionally, connecting to a nearer BS can yield a higher SINR, and thus achieve higher throughput. Capacity-based cell association schemes (CDA, SMBA, CDA&SMBA) achieve higher 50th, 80th and 90th percentile data rates than the Min-PL scheme. It is because

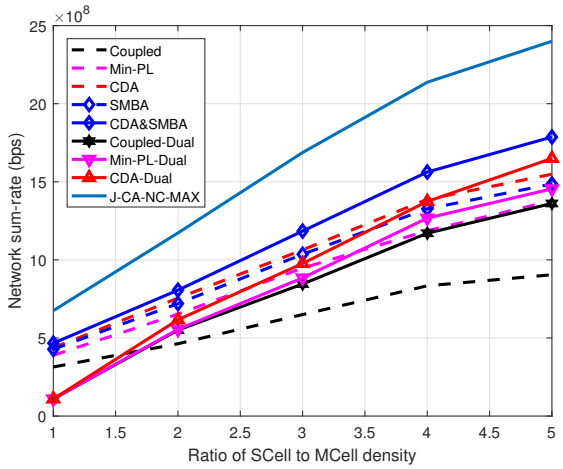

Fig. 6: Network sum-rate in the UL vs. ratio of SCell density to MCell density in single and dual connectivity scenarios ($\gamma = 0.5$).

SCells serve fewer UEs in this case than with Min-PL, though these UEs achieve higher data rates at the expense of the 10th and 20th percentile per UE data rates. Furthermore, for Min-PL, CDA and coupled schemes, dual-BS association can achieve higher 10th, 20th, 50th, 80th percentile data rates than single-BS association.

Fig. 6 shows the impact of varying the SCell density within the MCell coverage area on the UL network sum-rate. The densities of UEs and MCells remain constant across the different cases. As the number of deployed SCells increases, the network sum-rate grows. This is because adding more SCells means more UEs are offloaded from the MCell to the SCells where they are granted more resources compared to the resources offered by the congested MCells. Additionally, decoupled association schemes provide better performance in comparison with the coupled scheme. Furthermore, capacity-based association schemes (CDA, SMBA, CDA&SMBA) have higher network sum-rate than Min-PL which do not consider cell loads. It is worth noting that dual connectivity does not necessarily improve the sum-rate, especially when the number of BSs is small. An explanation for this could be that increasing the association pairs may increase interference and decrease the available RBs for the users near the BSs. Determining whether to increase the number of connections from the perspective of capacity gain seems more reasonable. Furthermore, CDA and Min-PL have a tangible effect in the single connectivity scenario, but for dual connectivity, its effect is limited. This may be because the frequency resource has been utilized efficiently in dual and hybrid connectivity. On the other hand, it is evident that the J-CA-NC-MAX scheme serves as an upper-bound to the network sum-rate due to the following reasons. First, the sum-rates of CDA and SMBA are dependent upon the initial association pairs, which are chosen to be the same as those in the UL, but in fact, they can also be set by the Min-PL scheme or randomly. In turn, different initial association pairs can lead to different final sum-rates. Second, the higher network sum-rate achieved by the J-CA-NC-MAX

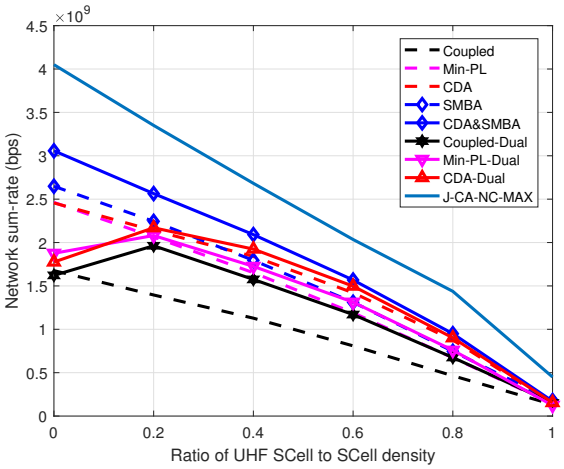

Fig. 7: Network sum-rate in the UL vs. ratio of UHF SCell density to SCell density in single and dual connectivity scenarios ($\beta = 5$).

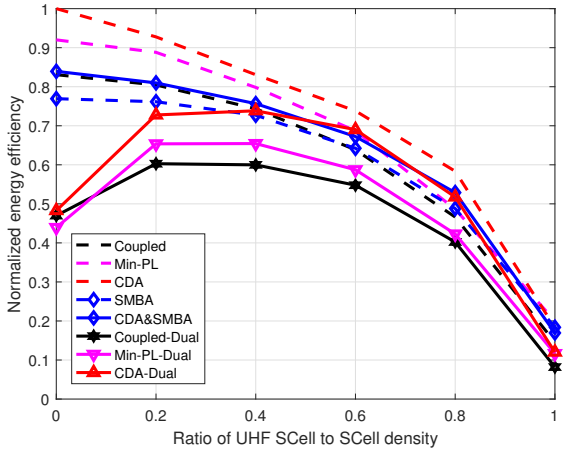

Fig. 8: Normalized network energy efficiency when the UHF SCells make up different proportions of all the SCells ($\beta = 5$).

scheme is at the expense of some UEs' data rates being lower, which impairs the fairness of the network UEs. However, for the CDA and SMBA schemes, the data rate of each UE will not be lower than the coupled association scheme.

Fig. 7 shows the UL network sum-rate when the UHF SCells make up different proportions of all the SCells. It can be seen that the different dual-BS association schemes follow a similar trend. Specifically, the sum-rate increases first and then decreases under different ratios of UHF SCell to total SCell densities. As might be anticipated, wireless networks with both UHF and mmWave SCells have better coverage than those with mmWave SCells. However, for the other association schemes, the network sum-rate decreases when the number of mmWave BSs decreases. This is because of the decrease in the bandwidth available. Moreover, CDA can achieve higher sum-rate in the single and dual hybrid connectivity scenario than in the dual connectivity scenario, and the advantage of decoupled association is less effective in the dual connectivity. This is due to the fact that the UEs distribution among the BSs is more balanced in the dual connectivity scenario.

Fig. 8 shows the UL energy efficiency when the UHF SCells make up different proportions of all the SCells. It can be seen that for the same association scheme, single connectivity is more energy efficient than dual connectivity, because the path-loss between a UE and its second serving BS is relatively higher. Moreover, in most cases, decoupled association schemes have higher energy efficiency than the coupled association scheme, since DUDe shortens the distance between UEs and BSs. The CDA scheme reconciles the RB utilization and interference, and thus, it has higher energy efficiency than the Min-PL scheme in the single and dual connectivity scenarios. For single connectivity and single-dual hybrid connectivity, the energy efficiency increases with the number of mmWave SCells. It is because there is almost no interference among mmWave UEs and when the density of mmWave SBSs is high, the directional antenna can compensate for the high path-loss of mmWave signals, and thus, the HetNet with more mmWave SBSs can achieve higher sum-rate. By contrast, the energy efficiency of the dual connectivity schemes increases first and then decreases. This is because mmWave signals are sensitive to blockage, and since the distance between a UE and its LOS mmWave serving BS can be long, deploying more UHF SBSs can shorten the UE-BS distance, but at the same time aggravate the co-channel interference.

Fig. 9 shows the number of handovers (switching among the serving BSs) for the different schemes, when there are 40 UEs, 1 MBS and at most 5 SBSs. The Min-PL and coupled association schemes can complete the BS association in one iteration. For CDA and SMBA, however, it takes a number of iterations to converge, though in the meantime, the UEs can connect to their DL serving BSs in the UL first, and in each iteration, only one association pair is changed without affecting the other existing associations. It can be seen from Fig. 9 that the number of handovers increases with the number of BSs. The CDA scheme requires more iterations to converge in the single connectivity scenario than in the dual connectivity scenario because the UEs distribution among the BSs is more balanced in the dual connectivity scenario.

B. Two-Tier mmWave-UHF HetNet

In order to promote system integration, we also consider the special case where all SBSs are of the same type, i.e., $\gamma = 1$ or $\gamma = 0$. Although many of the results are similar to those in the three-tier HetNet, there are some subtle differences. For HetNets consisting of UHF MCells and mmWave SCells (Fig. 10a), the ratio of mmWave SCell UE in the dual connectivity scenario is higher than that in the single connectivity scenario. Due to the high path-loss and blockage of mmWave, the coverage of mmWave SCell is smaller than that of UHF MCells in the UL. However, if there is only one MBS nearby then the second association pair must be with a mmWave SCell. Additionally, by comparing Fig. 10a with Fig. 10b, it is evident that the ratio of mmWave SCell is doubled, but the mmWave SCell UEs increase more than twice. This also

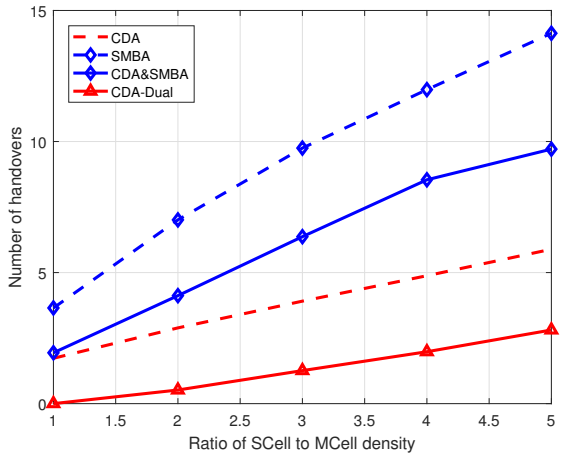

Fig. 9: Number of handovers in the UL vs. ratio of SCell density to MCell density in single and dual connectivity scenarios ($\gamma = 0.5$).

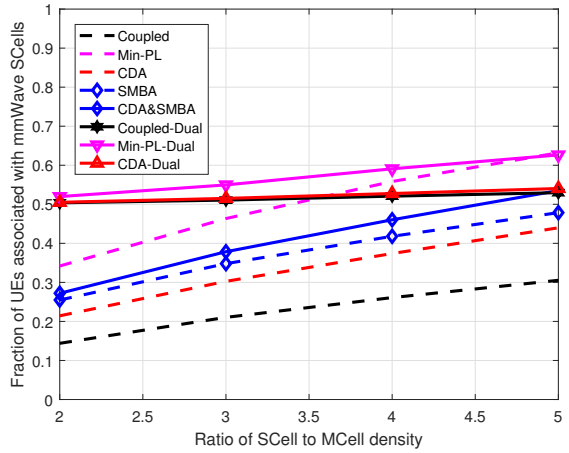

(a) $\gamma = 0$

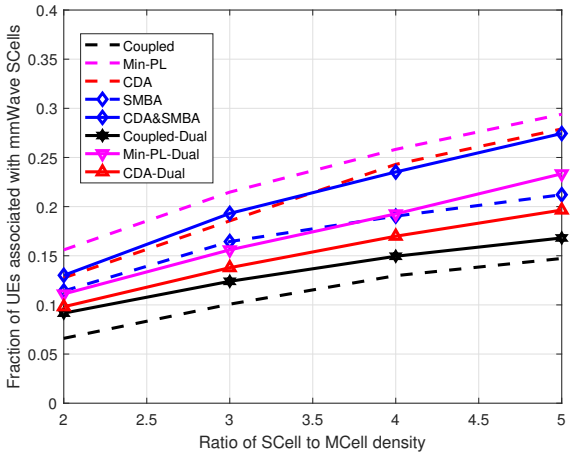

(b) $\gamma = 0.5$

Fig. 10: Ratio of UEs associated with mmWave SCells in the UL vs. ratio of SCell density to MCell density with different ratios of mmWave SCells.

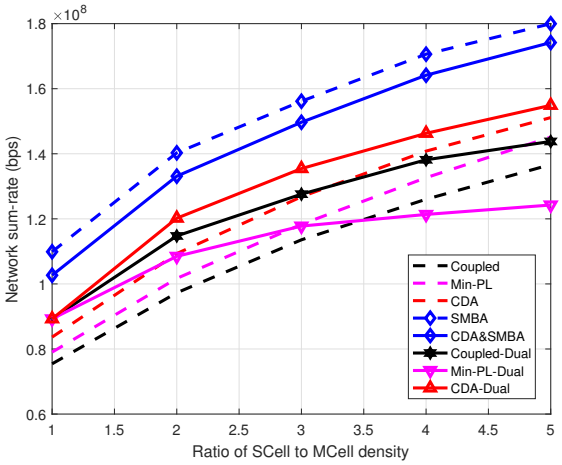

(a) $\gamma = 1$

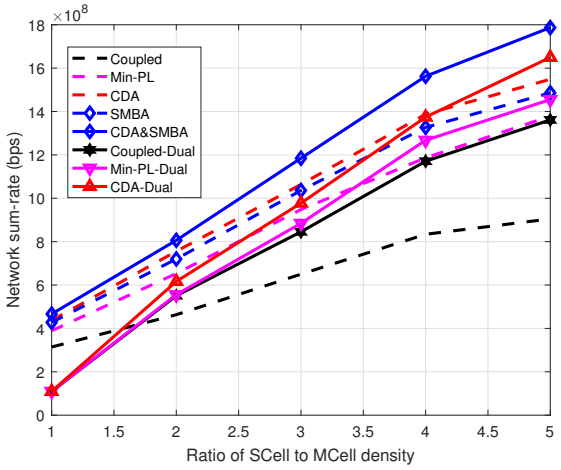

(b) $\gamma = 0.5$

Fig. 11: Network data rate in the UL vs. ratio of SCell to MCell density with different ratios of mmWave SCells.

verifies that the UEs prefer UHF BSs to mmWave SBSs when both are available.

Compared to Fig. 11b, it is obvious that the sum-rate of the HetNets with only UHF SCells (Fig. 11a) is much lower than those with mmWave SCells, and this is because the mmWave bandwidth is much wider than UHF bandwidth. Moreover, the sum-rate based on Min-PL, CDA and coupled schemes increases more slowly with the increase in the SCell to MCell density in the dual connectivity scenario than in the single connectivity scenario, which is different from the result in Fig. 11b. This is because increasing the number of BSs transmitting over UHF bands increases not only resource utilization but also collaterally interference, and the dual connectivity can make the interference even higher. Moreover, the sum-rate based on the coupled scheme is higher than the Min-PL scheme in the dual connectivity scenario. This is because a few UEs near SBSs acquire rich resources and thus achieve a very high data rate with the coupled scheme.

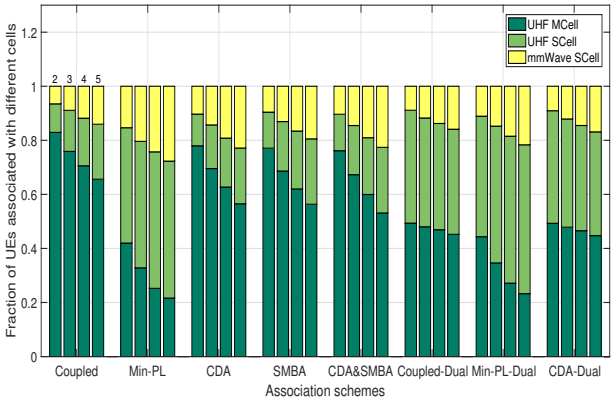

Fig. 12: Ratio of UEs associated with different BSs at different ratios of SCell density to MCell density and association schemes (less density scenario, $\gamma = 0.5$).

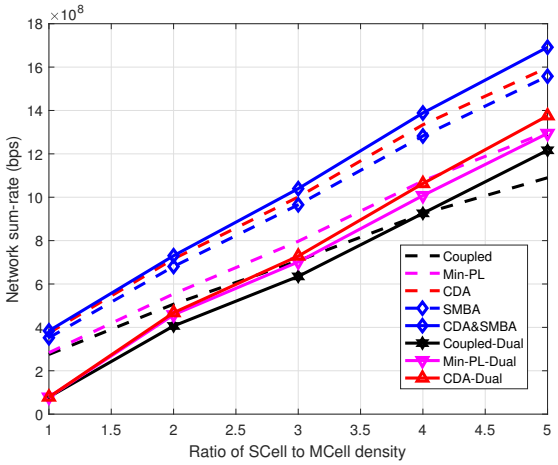

Fig. 13: Network sum-rate in the UL vs. ratio of SCell density to MCell density in single and dual connectivity scenarios (less density scenario, $\gamma = 0.5$).

C. Reduced Density Scenario

The BS and UE densities are reduced by half in Fig. 12, but the number of BSs and UEs is kept constant. Compared with Fig. 3, the number of UEs associated with the mmWave BSs decreases while the number of UEs associated with UHF BSs increases. When the BS density decreases, the average distance between UEs and BSs becomes longer, making it more difficult for UEs to access the mmWave BSs. Besides, compared with Fig. 6, the network sum-rate in Fig. 13 dropped due to the decreased BS density. Furthermore, the network sum-rate for the dual connectivity association schemes is severely degraded. It is because the distance to the second best BS becomes longer, thus connecting to a far away BS is not energy efficient and will decrease the available RBs for the UEs near the BSs. In these circumstances, the sum-rate of the CDA and SMBA schemes in the dual connectivity scenario is even lower than those in the single connectivity scenario.

V. Conclusion

This paper proposed a DUDe based resource allocation and multi-BS association technique to improve the performance of hybrid HetNets. Both capacity maximization and minimum path-loss based approaches were considered using single and dual connectivity. The results provide an insight into the performance of DUDe combined with mmWave and dual connectivity techniques for various performance metrics of interest. It was shown that capacity-based cell association schemes (CDA, SMBA, CDA&SMBA) can achieve higher data rates than path-loss based cell association. CDA scheme reconciles the RB utilization and interference, thus has higher energy efficiency than the Min-PL scheme in the single and dual connectivity scenarios. Moreover, it has been demonstrated that dual connectivity does not necessarily improve the sum-rate, especially when the density of UHF BSs is low. Determining whether to increase the number of connections from the perspective of capacity gain seems more reasonable. The advantage of decoupled association is less effective in dual connectivity, because the UEs distribution among the BSs is more balanced in the dual connectivity scenario than in the single connectivity scenario. Finally, the available mmWave bandwidth is much wider than UHF bandwidth, and so the network sum-rate mostly depends on the density of mmWave BSs, but UHF SBSs and MBSs are still important to provide umbrella coverage to guarantee a consistent service.

Acknowledgement

This work was partially supported by the Kuwait Foundation for the Advancement of Sciences (KFAS) under project code PN17-15EE-02.

References

[1] Boccardi, Federico, et al. "Why to decouple the uplink and downlink in cellular networks and how to do it," *IEEE Communications Magazine*, vol. 54, no.3, pp.110-117, 2015.

[2] Lopez-Perez, D., Guvenc, I., De, l. R. G., & Kountouris, M., "Enhanced intercell interference coordination challenges in heterogeneous networks," *IEEE Wireless Communications*, vol. 18, no. 3, pp. 22-30, 2011.

[3] H. Elshaer, F. Boccardi, M. Dohler, and R. Irmer, "Downlink and Uplink Decoupling: A disruptive architectural design for 5G networks," *IEEE Global Communications Conference (GLOBECOM)*, pp. 1798-1803, 2014.

[4] S. Singh, X. Zhang, and J. G. Andrews, "Joint Rate and SINR Coverage Analysis for Decoupled Uplink-Downlink Biased Cell Associations in HetNets," *IEEE Transactions on Wireless Communications*, vol. 14, no. 10, pp. 5360-5373, 2014.

[5] K. Smiljkovikj, P. Popovski, and L. Gavrilovska, "Analysis of the Decoupled Access for Downlink and Uplink in Wireless Heterogeneous Networks," *IEEE Wireless Communications Letters*, vol. 4, no. 2, pp. 173-176, 2015.

[6] Zhang, Lan, Weili Nie, Gang Feng, Fu-Chun Zheng, and Shuang Qin, "Uplink performance improvement by decoupling uplink/downlink access in HetNets," *IEEE Transactions on Vehicular Technology*, vol. 66, no. 8, pp. 6862-6876, 2017.

[7] Hemadeh, Ibrahim, et al., "Millimeter-wave communications: Physical channel models, design considerations, antenna constructions and link-budget," *IEEE Communications Surveys & Tutorials*, 2017.

[8] Pi Z, Khan F, "An introduction to millimeter-wave mobile broadband systems," *IEEE communications magazine*, vol. 49, no. 6, 2011.

[9] Azar, Yaniv, *et al.*, "28 GHz Propagation Measurements for Outdoor Cellular Communications Using Steerable Beam Antennas in New York City," *IEEE International Conference on Communications (ICC)*, pp. 5143-5147, 2013.

[10] T. S. Rappaport, J. N. Murdock, and F. Gutierrez, "State of the Art in 60-GHz Integrated Circuits and Systems for Wireless Communications," *Proceedings of the IEEE*, vol. 99, no. 8, pp. 1390-1436, 2011.
[11] Aylwin, "3G & 4G Frequency List". [Online]. Availabble: https://support.alwaysonlinewireless.com/, Accessed on: Feb. 28,2019.
[12] D. Colombi, B. Thors, and C. Trnevik, "Implications of EMF Exposure Limits on Output Power Levels for 5G Devices Above 6 GHz", *IEEE Antennas and Wireless Propagation Letters*, vol. 14, pp. 1247-1249, 2015.
[13] H. Elshaer, M. N. Kulkarni, F. Boccardi, J. G. Andrews, and M. Dohler, "Downlink and Uplink Cell Association With Traditional Macrocells and Millimeter Wave Small Cells," *IEEE Transactions on Wireless Communications*, vol. 15, no. 9, pp. 6244-6258, Sep. 2016.
[14] O. W. Bhatti *et al.*, "Performance Analysis of Decoupled Cell Association in Multi-tier Hybrid Networks Using Real Blockage Environments," *Wireless Communications and Mobile Computing Conference*, pp. 62-67, 2017.
[15] Chen, Zhilin, X. Hou, and C. Yang, "Training Resource Allocation for User-Centric Base Station Cooperation Networks." *IEEE Transactions on Vehicular Technology*, vol. 65, no. 4, pp. 2729-2735, 2016.
[16] S. Chandrashekar, A. Maeder, C. Sartori, T. Hhne, B. Vejlgaard, and D. Chandramouli, "5G Multi-RAT Multi-connectivity Architecture," *IEEE International Conference on Communications Workshops (ICC)*, pp. 180-186, 2016.
[17] A. Zakrzewska, D. Lopez-Perez, S. Kucera, and H. Claussen, "Dual Connectivity in LTE HetNets with Split Control- and User-Plane," *IEEE Global Communications Conference (GLOBECOM) Workshops*, pp. 391-396, 2013.
[18] S. C. Jha, K. Sivanesan, R. Vannithamby, and A. T. Koc, "Dual Connectivity in LTE small cell networks," *IEEE Global Communications Conference (Globecom) Workshops*, pp. 1205-1210, 2014.
[19] M. A. Lema, E. Pardo, O. Galinina, S. Andreev, and M. Dohler, "Flexible Dual-Connectivity Spectrum Aggregation for Decoupled Uplink and Downlink Access in 5G Heterogeneous Systems," *IEEE Journal on Selected Areas in Communications*, vol. 34, no. 11, pp. 2851-2865, Nov. 2016.
[20] J. Sangiamwong, Y. Saito, N. Miki, and T. Abe, "Investigation on Cell Selection Methods Associated with Inter-cell Interference Coordination in Heterogeneous Networks for LTE-Advanced Downlink," *Wireless Conference 2011 - Sustainable Wireless Technologies*, pp. 1-6, 2010.
[21] M. Sternad, T. Ottosson, A. Ahlen, and A. Svensson, "Attaining both coverage and high spectral efficiency with adaptive OFDM downlinks," *IEEE Vehicular Technology Conference (VTC)*, pp. 2486-2490, 2003.
[22] Samimi M K, MacCartney G R, Sun S, et al, "28 GHz millimeter-wave ultrawideband small-scale fading models in wireless channels," *Vehicular Technology Conference (VTC Spring)*, 2016 IEEE 83rd. IEEE, 2016: 1-6.
[23] Mathworks, "Multipath Fading Channel". [Online]. Avaliable: https://www.mathworks.com, Accessed on: Feb. 28, 2019.
[24] N. Kolehmainen, J. Puttonen, P. Kela, T. Ristaniemi, T. Henttonen, and M. Moisio, "Channel Quality Indication Reporting Schemes for UTRAN Long Term Evolution Downlink," *IEEE Vehicular Technology Conference (VTC)*, pp. 2522-2526, 2008.
[25] Minwei S , Kai Y , Chengwen X , et al, "Decoupled Heterogeneous Networks with Millimeter Wave Small Cells," *IEEE Transactions on Wireless Communications*, vol. 17, no. 9, pp. 5871-5884, 2018.
[26] Arnold, Oliver, et al., "Power consumption modeling of different base station types in heterogeneous cellular networks," *Future Network and Mobile Summit IEEE*, pp. 1-8, 2011.
[27] 3GPP, "Physical Layer Procedures," Sophia-Antipolis Cedex, France, TS 36.213.
[28] Berger, S, et al., "Dynamic Range-Aware Uplink Transmit Power Control in LTE Networks: Establishing an Operational Range for LTE's Open-Loop Transmit Power Control Parameters," *Wireless Communications Letters IEEE*, vol. 3, no. 5, 521-524, 2015.
[29] Ebrahim, A., E. Alsusa, and W. Pramudito, "Joint Interference Aware Resource Partitioning and Cellular Association for Femtocell Networks." *IEEE Global Communications Conference*, pp. 1-5, 2015.
[30] M. Fallgren, "On the complexity of maximizing the minimum Shannon capacity in Wireless Networks by joint channel assignment and power allocation," *International Workshop on Quality of Service*, pp. 1-7, 2010.
[31] M. Schlueter, "MIDACO software performance on interplanetary trajectory benchmarks", *Advances in Space Research*, vol. 54, no. 4, pp. 744754, 2014.
[32] Campos J., "Understanding the 5G NR Physical Layer," *Keysight technologies*, 2017.
[33] Zaidi A, Baldemair R, Andersson M, et al. "Designing for the future: the 5G NR physical layer," *Ericsson Technology Review*, 2017.
[34] 3GPP, "5G; NR; Base Station (BS) radio transmission and reception", TS 38.104, version 15.3.0, Release 15. [Online]. Available: http://www.3gpp.org/, Accessed on: Feb. 28,2019.
[35] "Percentile", Wikipedia. [Online]. Available: https://en.wikipedia.org/wiki/Percentile, Accessed on: Oct. 31, 2018.

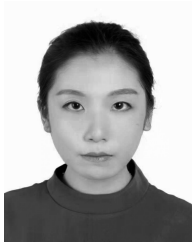

Yao Shi received her M.Sc. degree in information and communication engineering from Harbin Institute of Technology, China, in 2017. She is currently working toward the Ph.D. degree in electrical and electronic engineering, University of Manchester, UK. Her research interests include wireless communications and networking, resource allocation and management, and green and energy-harvesting networks.

Emad Alsusa (SM'07) received the Ph.D. degree in telecommunications from the University of Bath in 2000. In 2000, he became a Post-Doctoral Research Associate with Edinburgh University. He joined Manchester University in 2003, as a Full Faculty Member. His research interest lies in the area of signal processing and communication theory with a focus on the physical and MAC layers of wireless communication networks for which he designs advanced algorithms for energy and spectrum optimization in the presence of interference and various channel nonlinearities. His research work has so far resulted in well over a 150 journal and refereed conference publications mainly in the top IEEE venues. He is a fellow of the U.K. Higher Academy of Education. He has volunteered for various IEEE activities, including the VTC TPC Co-Chair of the Greencom Track in VTC 2016 and the General Co-Chair of the Online Green Com Conference in 2016.

Aysha Ebrahim received the B.Sc. degree in computer engineering from University of Bahrain in 2009, the M.Sc. degree in electronic engineering from University of York in 2011, and the Ph.D. degree in electrical and electronic engineering from The University of Manchester in 2016. She is currently with the Department of Computer Engineering, University of Bahrain, as an Assistant Professor. Her research focuses on radio resource management techniques for heterogeneous wireless networks.

Mohammed W. Baidas (M'05-SM'17) received the B.Eng. (first class honors) degree in communication systems engineering from the University of Manchester, Manchester, U.K., in 2005, the M.Sc. degree with distinction in wireless communications engineering from the University of Leeds, Leeds, U.K., in 2006, the M.S. degree in electrical engineering from the University of Maryland, College Park, MD, USA in 2009, and the Ph.D. degree in electrical engineering from Virginia Tech, Blacksburg, VA, USA, in 2012. Dr. Baidas is a frequent reviewer for several IEEE and international journals and conferences, with over 50 publications. He is currently an Associate Professor at the Department of Electrical Engineering, Kuwait University, Kuwait, where he has been on the faculty since May 2012. His research interests include resource allocation and management in cognitive radio systems, game theory, cooperative communications and networking, and green and energy-harvesting networks.